the FEBS Journal

Importance of tyrosine residues of *Bacillus stearothermophilus* serine hydroxymethyltransferase in cofactor binding and L-*allo*-Thr cleavage

Crystal structure and biochemical studies

B. S. Bhavani[1,*], V. Rajaram[2,*], Shveta Bisht[2], Purnima Kaul[1], V. Prakash[1], M. R. N. Murthy[2], N. Appaji Rao[3] and H. S. Savithri[3]

1 Protein Chemistry and Technology, Central Food Technological Research Institute, Mysore, India
2 Molecular Biophysics Unit, Indian Institute of Science, Bangalore, India
3 Department of Biochemistry, Indian Institute of Science, Bangalore, India

Keywords
crystal structure; proton abstraction; pyridoxal 5′-phosphate-dependent enzymes; serine hydroxymethyltransferase; tetrahydrofolate-independent cleavage

Correspondence
H. S. Savithri, Department of Biochemistry, Indian Institute of Science, Bangalore-560 012, India
Fax: +91 80 2360 0814
Tel: +91 80 2293 2310
E-mail: bchss@biochem.iisc.ernet.in

*These authors contributed equally to this work

(Received 8 May 2008, revised 4 July 2008, accepted 18 July 2008)

doi:10.1111/j.1742-4658.2008.06603.x

Serine hydroxymethyltransferase (SHMT) from *Bacillus stearothermophilus* (bsSHMT) is a pyridoxal 5′-phosphate-dependent enzyme that catalyses the conversion of L-serine and tetrahydrofolate to glycine and 5,10-methylene tetrahydrofolate. In addition, the enzyme catalyses the tetrahydrofolate-independent cleavage of 3-hydroxy amino acids and transamination. In this article, we have examined the mechanism of the tetrahydrofolate-independent cleavage of 3-hydroxy amino acids by SHMT. The three-dimensional structure and biochemical properties of Y51F and Y61A bsSHMTs and their complexes with substrates, especially L-*allo*-Thr, show that the cleavage of 3-hydroxy amino acids could proceed via Cα proton abstraction rather than hydroxyl proton removal. Both mutations result in a complete loss of tetrahydrofolate-dependent and tetrahydrofolate-independent activities. The mutation of Y51 to F strongly affects the binding of pyridoxal 5′-phosphate, possibly as a consequence of a change in the orientation of the phenyl ring in Y51F bsSHMT. The mutant enzyme could be completely reconstituted with pyridoxal 5′-phosphate. However, there was an alteration in the λ_{max} value of the internal aldimine (396 nm), a decrease in the rate of reduction with $NaCNBH_3$ and a loss of the intermediate in the interaction with methoxyamine (MA). The mutation of Y61 to A results in the loss of interaction with Cα and Cβ of the substrates. X-Ray structure and visible CD studies show that the mutant is capable of forming an external aldimine. However, the formation of the quinonoid intermediate is hindered. It is suggested that Y61 is involved in the abstraction of the Cα proton from 3-hydroxy amino acids. A new mechanism for the cleavage of 3-hydroxy amino acids via Cα proton abstraction by SHMT is proposed.

Serine hydroxymethyltransferase (SHMT) plays an important role in both amino acid and nucleotide metabolism by providing one-carbon units for the biosynthesis of purines, thymidylate, methionine and choline [1]. SHMT is also considered to be an important target for cancer chemotherapy [2]. It catalyses the

Abbreviations
bsSHMT, *Bacillus stearothermophilus* SHMT; eSHMT, *Escherichia coli* SHMT; FTHF, 5-formyl-THF; LB, Luria–Bertani; MA, methoxyamine; mcSHMT, murine cytosolic SHMT; PLP, pyridoxal 5′-phosphate; rcSHMT, rabbit liver cytosolic SHMT; scSHMT, sheep liver cytosolic SHMT; SHMT, serine hydroxymethyltransferase; THF, tetrahydrofolate.

reversible interconversion of L-Ser and tetrahydrofolate (THF) to Gly and 5,10-methylene THF. In addition, it catalyses the THF-independent cleavage of L-*allo*-Thr, transamination, decarboxylation and racemization reactions [3–5]. SHMT belongs to the α-family of pyridoxal 5′-phosphate (PLP)-dependent enzymes. The reversible conversion of L-Ser to Gly proceeds via several intermediates with distinct absorption maxima, which have aided in the elucidation of the reaction mechanism [2].

In an earlier study, we determined the structures of *Bacillus stearothermophilus* SHMT (bsSHMT) and its binary and ternary complexes [6]. Figure 1 depicts the geometry of the active site of the bsSHMT–Ser external aldimine, highlighting the residues that may be involved in catalysis. A retro-aldol cleavage mechanism (Scheme 1A) has been proposed previously for the L-Ser cleavage, in which the reaction begins with an abstraction of a proton from the hydroxymethyl group. However, structural and mutational studies on the active site glutamate [E74 of sheep liver cytosolic SHMT (scSHMT) [7], E53 of bsSHMT [8] and E75 of rabbit liver cytosolic SHMT (rcSHMT) [9]] have shown that the THF-dependent conversion of L-Ser to Gly is completely abolished in these mutants. However, the THF-independent cleavage of L-*allo*-Thr is enhanced several fold, clearly suggesting that glutamate is not involved in the proton abstraction from 3-hydroxy amino acids. It has been shown that the glutamate residue is involved in the appropriate positioning of L-Ser [7,8]. The loss of physiological activity has been attributed to the loss of interaction of E53 with THF [8]. Mutation of H147 in scSHMT (corresponding to H122 in bsSHMT) does not result in a considerable loss of THF-dependent and THF-independent activities [10]. Hence, it is unlikely to be the residue involved in proton abstraction from the hydroxyl group of L-Ser and other 3-hydroxy amino acids. A detailed examination of the binary and ternary complexes of bsSHMT has enabled us to propose a direct displacement mechanism (Scheme 1B) for the THF-dependent cleavage of L-Ser, in which a nucleophilic attack by N5 of THF facilitates Cα–Cβ bond cleavage of L-Ser accompanied by the release of a water molecule to form the product (Gly quinonoid intermediate), and THF is converted to 5,10-methylene THF [6] (Scheme 1B). Clearly, the same mechanism may not hold good for the THF-independent reaction catalysed by SHMT.

Active site Lys and Tyr residues have been invoked as Cα proton abstractors in several PLP-dependent enzymes, such as aspartate aminotransferase [11,12], 5-aminolaevulinate synthase [13] and alanine racemase [14]. Structural and mutational analysis of the active site Lys mutant K226M bsSHMT demonstrated that Lys was not involved in Cα proton abstraction [15]. As evident from Fig. 1, Y51 and Y61 are the other possible candidates for Cα proton abstraction. Sequence comparison of SHMT from various sources has revealed that Y51, Y60 and Y61 (numbering according to bsSHMT) are well conserved. In the internal aldimine structure of bsSHMT, the hydroxyl group of Y51 is found to interact with the phosphate group of PLP (Fig. 1), and the side-chain of Y61 is hydrogen bonded to R357 (2.7 Å) and points away from E53 (5 Å). In the external aldimine structure, Y61 points towards E53, approaching its side-chain carboxylate group and Cβ of the bound ligand, L-Ser (2.8 Å) [6]. The residues corresponding to Y61 of bsSHMT in scSHMT (Y82) [7] and eSHMT (Y65) [16] have been mutated to F previously. Studies on these mutants have suggested that this residue may be involved in proton abstraction, stabilization of the quinonoid intermediate [7] and conversion of a closed to an open form of the enzyme [16].

Although extensive studies have been carried out on the mechanism of the THF-dependent reaction of SHMT, not much is known about the mechanism of

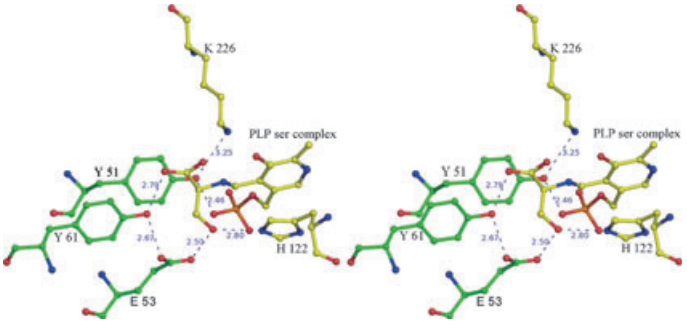

Fig. 1. Active site geometry of bsSHMT–Ser complex depicting the residues involved in catalysis. The stereo diagram of the bsSHMT–Ser active site shows the Schiff base between PLP and the amino group of L-Ser. Residues from the same subunit are shown in yellow and those from the other subunit in green. E53 and H122 interact with the hydroxyl group of L-Ser, Y51 interacts with the phosphate group of PLP and Y61 is close to Cβ of L-Ser.

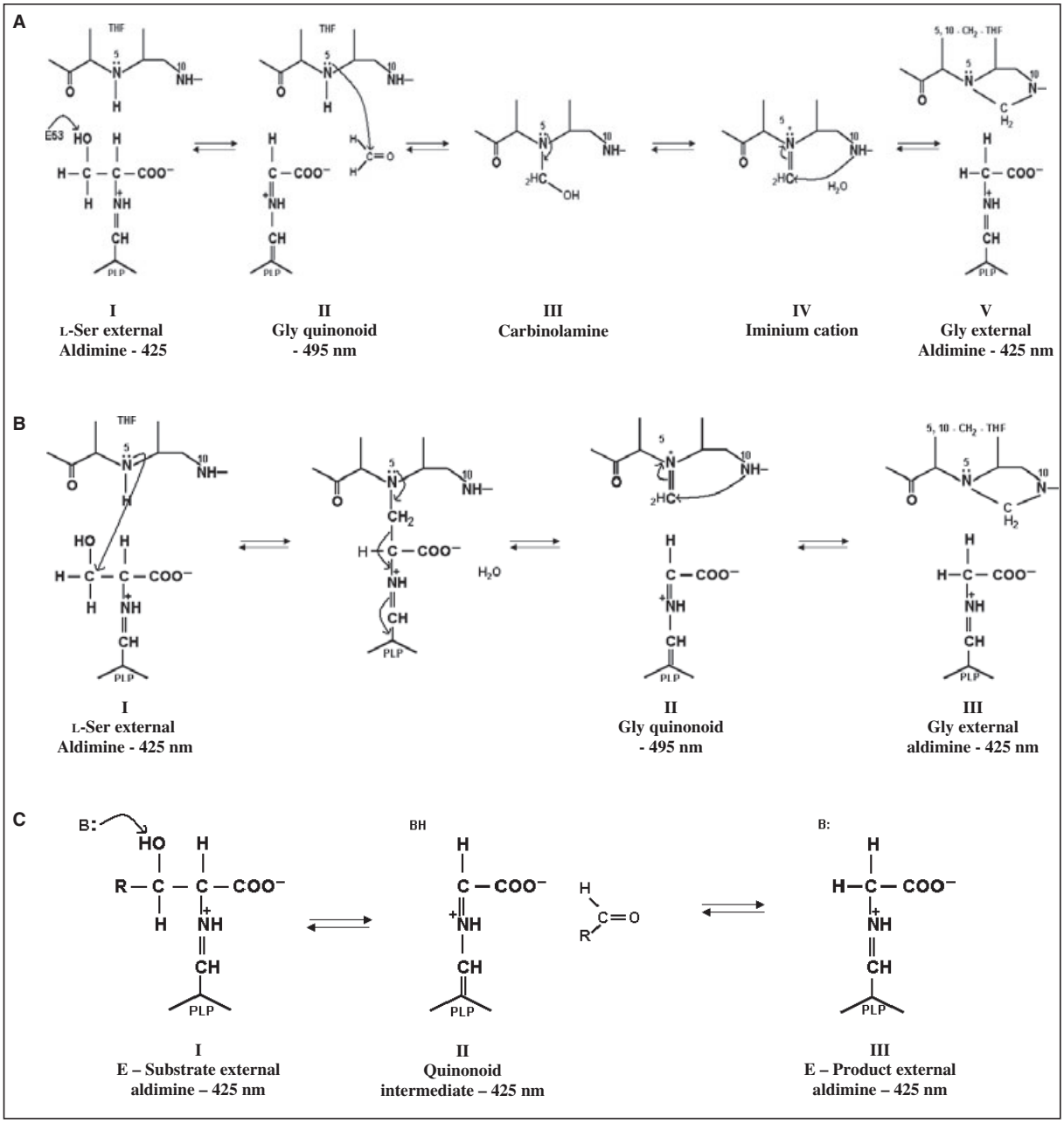

Scheme 1. Reaction mechanisms proposed for THF–dependent cleavage of L-Ser and THF-independent cleavage of 3-hydroxy amino acids by SHMT. (A) Retro-aldol mechanism. (B) Direct displacement mechanism. (C) Retro-aldol mechanism for the cleavage of 3-hydroxy amino acids.

the THF-independent cleavage of 3-hydroxy amino acids. Clearly, E53 and H122 or K226 are not involved in proton abstraction. It is possible that cleavage occurs by a mechanism different from the classical retro-aldol cleavage (Scheme 1C) [17]. In this article, we describe structural and functional studies on Y51F, Y61F and Y61A bsSHMTs. These studies suggest that Y61 is a possible candidate for proton abstraction from Cα of Gly and 3-hydroxy amino acids, and that Y51 is involved in PLP binding. An alternative mechanism, for the cleavage of 3-hydroxy amino acids via the abstraction of a Cα proton rather than a hydroxyl proton, is proposed.

Results and Discussion

PLP content and activity measurements of Y51F, Y61A and Y61F bsSHMTs

The purified Y51F and Y61F bsSHMTs were nearly colourless and pale yellow, respectively, indicating differences in the PLP content of these preparations (0.2 mol per mol of subunit in Y51F and 0.6 mol per mole of subunit in Y61F bsSHMT, compared with 1 mol per mole of subunit in bsSHMT). The PLP content of Y61A bsSHMT was similar to that of bsSHMT. The addition of 200 μM of PLP to the Y51F and Y61F bsSHMTs (1 mg·mL^{-1}) in buffer D, followed by incubation at 4 °C for 45 min and dialysis against buffer not containing PLP, restored the PLP content to 1 mol per mole of subunit. These observations suggest that PLP is lost during the purification of Y51F and Y61F bsSHMTs and can be restored completely on reconstitution. All further experiments were carried out with the reconstituted enzyme. The THF-dependent cleavage of L-Ser was completely abolished in all the mutants. When the activity was checked with L-*allo*-Thr under the conditions used for bsSHMT, no measurable activity could be detected. However, on increasing the enzyme concentration 100-fold, a barely detectable level of activity could be measured for Y61A bsSHMT. The transamination reaction with D-Ala was completely abolished in all the mutants. The results of activity measurements are summarized in Table 1. The kinetic parameters, such as K_m and V_{max}, for the mutant enzymes could not be determined because of their negligible activity.

Spectral and structural properties

Internal aldimine

The visible absorption spectrum of Y61A bsSHMT (Fig. 2A) was similar to that of bsSHMT, with maximum absorbance at 425 nm (Fig. 2A, inset). This corresponds to the internal aldimine form. In contrast, Y51F and Y61F bsSHMT mutants showed a λ_{max} value at 396 nm (Fig. 2B). Similar spectral changes were observed in the Y121F mutant of 5-aminolaevulinate synthase [13], K258H aspartate aminotransferase [11], K226M bsSHMT [15] and K229R eSHMT [18]. As Y51F and Y61F bsSHMTs showed a λ_{max} value different from that of the wild-type enzyme, the mode of PLP interaction in these mutants was examined further. $NaCNBH_3$ specifically reduces the internal

Table 1. Enzymatic activities of bsSHMT and its Tyr mutants.

Enzyme	Specific activity (L-Ser)[a]	Specific activity (L-*allo*-Thr)[b]	Transamination (D-Ala)[c] (s^{-1})
bsSHMT	5.0	0.65	0.04
Y51F	NDA[d]	NDA[d]	NDA[d]
Y61F	NDA[d]	NDA[d]	NDA[d]
Y61A	0.05	0.03	NDA[d]

[a] Micromoles of HCHO per minute per milligram when L-Ser and THF were used as substrates. [b] Micromoles of CH_3CHO per minute per milligram with L-*allo*-Thr as substrate. [c] Pseudo-first-order rate constant. [d] No detectable activity.

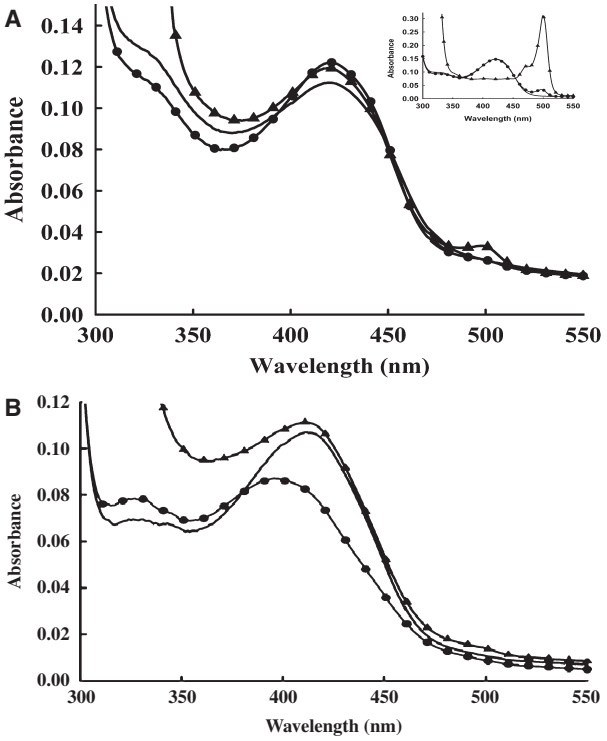

Fig. 2. (A) Absence of spectral changes in Y61A bsSHMT on addition of Gly or Gly + FTHF. Absorption spectra of Y61A bsSHMT (1 mg·mL^{-1}) in final buffer D (●) and on addition of 50 mM of L-Ser/Gly (—). Further addition of 1.8 mM/1 mM THF/FTHF results in a small amount of quinonoid intermediate at 495 nm (▲). Inset: spectrum of bsSHMT (1 mg·mL^{-1}) in buffer D (—) showing the absorption maximum at 425 nm, a characteristic of the PLP internal aldimine. The addition of Gly (50 mM) results in a spectrum with an additional small peak at 495 nm caused by formation of the quinonoid intermediate (●); further addition of THF (1.8 mM) enhances the concentration of the quinonoid intermediate (▲) with a concomitant loss of absorbance at 425 nm. (B) Spectral changes observed on addition of Gly or Gly/FTHF to Y51F bsSHMT. The spectrum of Y51F bsSHMT (1 mg·mL^{-1}) in buffer D (●) shows an absorption maximum at 396 nm; on addition of 50 mM L-Ser/Gly (—), the absorption maximum shifts to 412 nm; further addition of 1 mM THF/FTHF (▲) does not result in quinonoid intermediate formation. Y61F bsSHMT also shows similar results, but the data were not included to avoid repetition.

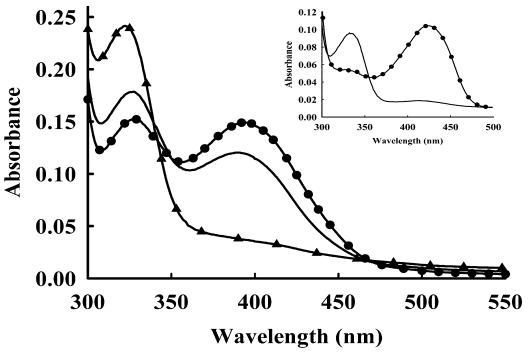

Fig. 3. The reduction of bsSHMT and Y51F bsSHMT on addition of $NaCNBH_3$. Spectrum of Y51F bsSHMT (1 mg·mL^{-1}) (●); spectra on addition of $NaCNBH_3$ (1 mM) after 5 min (—) and 30 min (▲). Inset: bsSHMT untreated (●) and 5 min after addition of $NaCNBH_3$ (—).

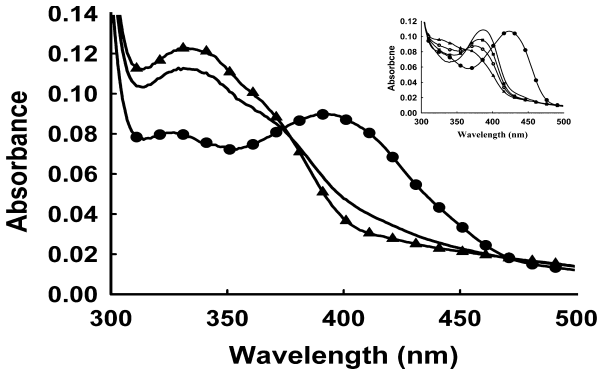

Fig. 4. Interaction of bsSHMT and Y51F bsSHMT with MA. Spectrum of Y51F bsSHMT (●); on addition of MA (10 mM), there is a marked decrease in absorbance at 396 nm in 2 min (—) and 20 min (▲). There is a concomitant increase in absorbance at 325 nm. Only the Y51F spectrum is given to avoid repetition, as all mutants gave similar results. Inset: interaction of MA with bsSHMT (●); MA (2 mM) was added and the spectra were recorded after 30 s (—), 10 min (■) and 20 min (▲). The figure shows the formation of an intermediate with an absorption maximum at 388 nm prior to the formation of the product oxime absorbing at 325 nm.

aldimine to a secondary amine [19]. In bsSHMT, this reaction proceeds to completion in 5 min (Fig. 3, inset). Although Y51F and Y61F bsSHMTs could be reduced by $NaCNBH_3$, the time required for completion of the reaction was 30 min (data for Y61F bsSHMT not shown) (Fig. 3). The addition of MA to bsSHMT results in its conversion to an oxime absorbing at 325 nm through an intermediate absorbing at 388 nm. The intermediate is formed in 30 s and the overall reaction takes 20 min to reach completion [20]. This intermediate is believed to be PLP (Fig. 4, inset). Any disruption at the active site results in the loss of this intermediate [15,21]. In all three mutants, the addition of MA results in the formation of the oxime in approximately the same time (20 min). However, the peak at 388 nm, corresponding to the formation of the intermediate, is not observed (Fig. 4). The rate constant for the conversion of the bsSHMT internal aldimine to the intermediate is 1.6 s^{-1} and the rate of conversion of the intermediate to the final product is 4×10^{-3} s^{-1}. The formation of the oxime in the mutants occurs with similar rate constants of 5×10^{-3} s^{-1} for Y51F, 2×10^{-3} s^{-1} for Y61F and 1×10^{-3} s^{-1} for Y61A bsSHMT. Thus, the mutants were able to interact with MA without forming an intermediate. These results suggest that the mutant enzymes are in an internal aldimine form; however, the environment of PLP is different.

The overall internal aldimine structures of Y51F and Y61A bsSHMTs are very similar to that of bsSHMT, with rmsd of 0.11 and 0.19 Å, respectively for the superposition of all Cα atoms. In bsSHMT, the Y51 hydroxyl group forms a hydrogen bond with the phosphate oxygen of PLP. In Y51F bsSHMT, this interaction is lost and the phenyl plane of F51 is rotated by 75° when compared with that of Y51. PLP is easily lost from Y51F as a result of this mutation. A water molecule is present in Y51F bsSHMT at the position corresponding to the hydroxyl of Y51. The change in the orientation of F51 in the mutant induces a corresponding change in the orientation of the phenyl ring of Y61 by about 85° (Fig. 5). A smaller change (18°) is also observed in the orientation of Y60. However, this change in orientation is probably a result of the change in ψ angle for the Y60–Y61 peptide unit by about 26°. There is a small change in the orientation of E53; no other significant changes were observed in Y51F bsSHMT. In spite of these changes, the orientation of PLP in Y51F bsSHMT is the same as that of bsSHMT. Most of the observed changes appear to result from the loss of stabilizing interactions caused by the Y to F mutation. These changes may account for the shift of the absorption maximum of the internal aldimine from 425 to 396 nm in the mutant (Fig. 2B), the loss of the characteristic ellipticity maximum at 425 nm for Y51F bsSHMT (Fig. 6) and the absence of intermediate (Fig. 4) on interaction with MA. Similar spectral changes are observed in Y61F bsSHMT. As this mutant did not crystallize, the related structural changes could not be ascertained.

In Y61A bsSHMT, the orientation of PLP is different by about 11° along the N1–C3 axis when compared with that of bsSHMT (data not shown). However, there is no change in the λ_{max} value of this mutant (425 nm, Fig. 2A). In addition, there are no significant changes in the orientation of residues E53,

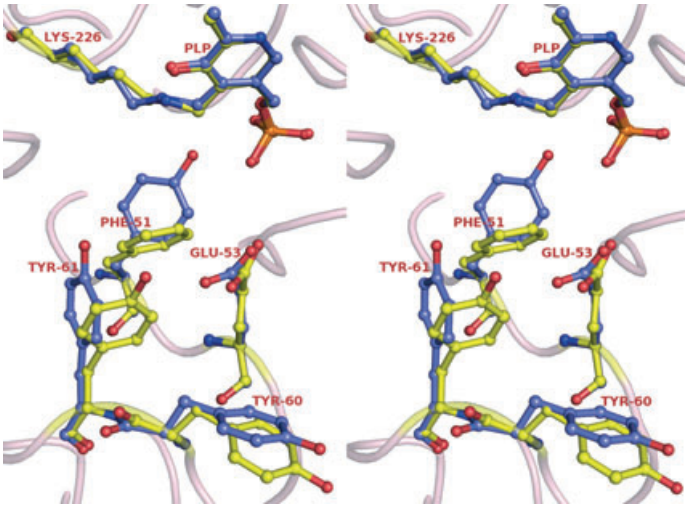

Fig. 5. Superposition of the active sites of bsSHMT (blue) and Y51F bsSHMT (yellow) showing the differences in the conformation of residues Y/F51, E53, Y60 and Y61.

Y51 and Y60 when compared with bsSHMT. In contrast, the spectral changes are minimal in Y61A bsSHMT when compared with Y51F and Y61F bsSHMTs. This is also reflected in the crystal structure of the Y61A bsSHMT internal aldimine (figure not shown).

Binary complex with Gly/L-Ser

The addition of L-Ser or Gly to Y51F and Y61F bsSHMTs results in a shift of the λ_{max} value from 396 to 412 nm (Fig. 2B, data not shown for Y61F bsSHMT). There is no change in the λ_{max} value when these ligands are added to Y61A bsSHMT, unlike that of bsSHMT (Fig. 2A). The addition of THF or 5-formyl-THF (FTHF) to the Gly external aldimine of bsSHMT converts a large fraction of the molecules to the quinonoid form, with an absorption maximum at 495 nm (Fig. 2A, inset) [7]. However, the addition of THF or FTHF to the Gly external aldimine of Y51F and Y61F bsSHMTs does not show the appearance of a 495 nm peak (Fig. 2B), and Y61A bsSHMT shows a barley detectable peak (0.8%) (Fig. 2A). This suggests that the formation of the quinonoid intermediate is affected in all three mutants.

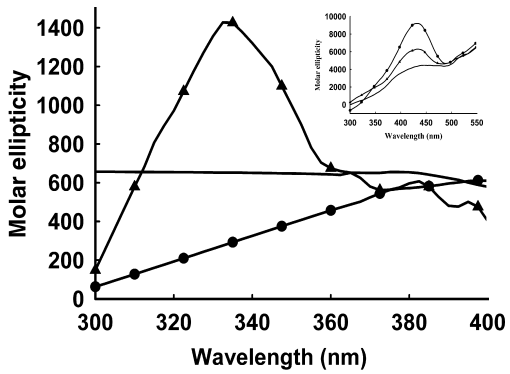

Fig. 6. Changes in the visible CD spectrum of Y51F and Y61A bsSHMT on addition of L-Ser/Gly. The visible CD spectrum of Y51F bsSHMT (●) (1 mg·mL^{-1}) shows no characteristic ellipticity maximum. However, on addition of Gly (▲), an ellipticity maximum is observed at 343 nm, suggesting the formation of a gem-diamine; the addition of 50 mM L-Ser does not produce a similar change (—). Inset: the visible CD spectrum of Y61A bsSHMT (1 mg·mL^{-1}) (●) shows an ellipticity maximum at 425 nm; the addition of 50 mM of L-Ser (—) or Gly (▲) results in a decrease in the ellipticity maximum of Y61A bsSHMT, suggesting the formation of an external aldimine.

The visible CD ellipticity maximum at 425 nm of bsSHMT is reduced on formation of the external aldimine with L-Ser or Gly [7]. Y61A bsSHMT exhibits similar spectral characteristics (Fig. 6, inset). No CD ellipticity is observed in the visible region with Y51F or Y61F bsSHMT mutants. The addition of L-Ser does not result in the appearance of any new CD peak. However, the addition of Gly to Y51F bsSHMT results in the appearance of a peak at 333 nm. This peak indicates the formation of a gem-diamine [8] (Fig. 6).

Although the overall structure of Y51F bsSHMT–Gly is very similar to that of bsSHMT–Gly, with an rmsd of 0.15 Å for the superposition of all Cα atoms, significant differences were observed in the PLP orientation and ligand binding properties. In the Y51F bsSHMT–Gly complex, PLP is found in its gem-diamine form, which is consistent with the observation of a visible CD ellipticity maximum at 333 nm (Fig. 6). However, the density connecting PLP and Gly is weaker than that connecting PLP and Lys (Fig. 7), and only the carboxyl of Gly has good density. These observations, coupled with spectroscopic studies,

suggest that the structure corresponds to the gem-diamine form. The conformations of F51, Y60, Y61 and E53 are very similar in Y51F and Y51F bsSHMT–Gly, although they are different from those seen in wild-type internal and external aldimines.

Another interesting observation is that the phosphate group of PLP is in two distinct conformations (Fig. 7). The additional conformation may be attributed to the loss of hydrogen bonding between Y51F and the phosphate oxygen. A few water molecules could be fitted with partial occupancy close to the oxygen atoms of the original phosphate. As a result of these changes, PLP orientation is also different in Y51F bsSHMT–Gly when compared with that of the wild-type internal and Gly external aldimine. The plane of the pyridine ring is rotated by about 22° along the C2–N1 axis. As a consequence, the C5A atom of PLP moves by 1.66 Å. The change in the orientation of PLP and the conformation of F51, Y60, Y61 and E53 could lead to Gly being present predominantly in the gem-diamine form (Figs 6 and 7).

In the Y61A bsSHMT–Gly complex, Gly is bound to PLP as an external aldimine. The position of Gly and orientation of PLP are very similar to those of the bsSHMT–Gly complex. Y61A bsSHMT crystallizes in the presence of Gly and FTHF in two forms, orthorhombic and monoclinic, with almost identical unit cell parameters. However, in both forms, no electron density is observed for FTHF. This is in contrast with the result obtained with bsSHMT, where co-crystallization with Gly and FTHF results in crystals of the ternary complex in a lower symmetric monoclinic form. The superposition of Y61A bsSHMT–Gly and bsSHMT–Gly–FTHF shows that the mutation of Y61 to A creates a large cavity near the binding site of the pteridine ring of FTHF, and this may affect the binding of FTHF/THF. The crystal structures of the Y51F and Y61A bsSHMT–Ser complexes show that L-Ser forms a clear external aldimine with PLP. The conformations of F51 and Y61 in Y51F bsSHMT–Ser are similar to those of Y51F bsSHMT–Gly. The external aldimine may be stabilized by interactions of the L-Ser hydroxyl group with E53 and the surrounding water molecules.

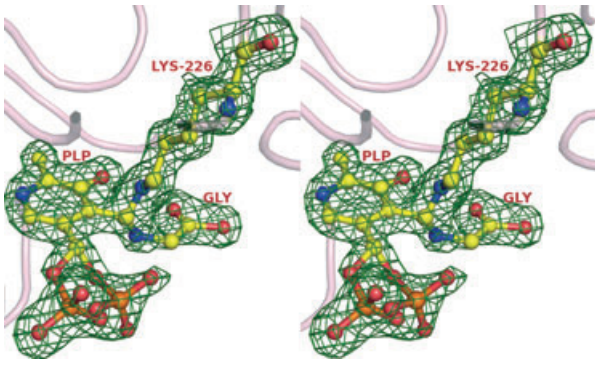

Fig. 7. Stereo diagram showing the electron density of the Y51F bsSHMT gem-diamine. Electron density (F_o–F_c, contoured at 3σ) for the gem-diamine of the Y51F bsSHMT–Gly complex. PLP is bonded to both K226 and Gly amino groups. The phosphate group is in double conformation.

L-*allo*-Thr complex

In bsSHMT, L-*allo*-Thr is cleaved to Gly, and hence the density corresponding to Gly only is observed when crystals are obtained in the presence of L-*allo*-Thr. The most interesting observation in these mutants is that an intact L-*allo*-Thr is bound to PLP and forms an external aldimine. Except for the bound ligand, the structures of the Y51F and Y61A bsSHMT–L-*allo*-Thr complexes (Fig. 8A,B) are very similar to that of bsSHMT–Gly(*allo*-Thr) (crystals of bsSHMT obtained in the presence of L-*allo*-Thr), with rmsd of 0.11 and 0.19 Å, respectively. The position and orientation of L-*allo*-Thr are similar to those of L-Ser in Y51F and Y61A bsSHMT–Ser complexes, with Oγ interacting with E53 and H122 (Fig. 8A). Cγ of L-*allo*-Thr has a hydrophobic interaction with the side-chain of S172.

In the Y51F bsSHMT-*allo*-Thr complex, the phosphate of PLP is in two conformations, as in Y51F bsSHMT–Gly. In Y61A bsSHMT, the density for the side-chain of L-*allo*-Thr is weaker than that for Y51F bsSHMT-*allo*-Thr. These are the first two mutants of SHMT in which L-*allo*-Thr is bound to PLP as an external aldimine and is not further converted to Gly and acetaldehyde. Mutation of Y51 and Y61 leads to the loss of the THF-independent reaction. Therefore, these residues may be directly involved in L-*allo*-Thr to Gly conversions.

Mechanism of THF-independent cleavage of L-*allo*-Thr by bsSHMT

The conversion of L-Ser to Gly by SHMT takes place in the presence of THF by a direct displacement mechanism [6]. The cleavage of L-*allo*-Thr to Gly is THF independent. The main difference between L-Ser and L-*allo*-Thr is the substitution of the Cβ hydrogen in L-Ser by a methyl group in L-*allo*-Thr. It has been proposed previously that the THF-independent conversion of β-hydroxy amino acids, such as L-*allo*-Thr, by SHMT takes place by a retro-aldol cleavage mechanism (Scheme 1C) [17]. In this mechanism, the first step is the abstraction of a proton from the side-chain hydroxyl group. The crystal structure of the bsSHMT–

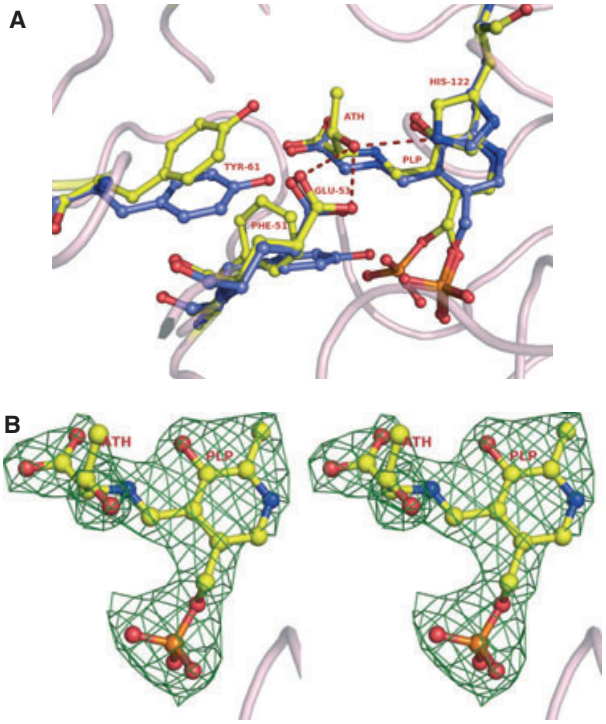

Fig. 8. (A) Superposition of the active sites of Y51FbsSHMT (yellow) and bsSHMT (blue) complexes obtained in the presence of L-*allo*-Thr. The interactions of L-*allo*-Thr with E53 and H122 in Y51FbsSHMT-*allo*-Thr (yellow) are shown as dotted lines. (B) Electron density (F_o–F_c, contoured at 3σ) corresponding to L-*allo*-Thr in Y61A bsSHMT.

Ser complex suggests that H122 and E53 are well positioned for abstracting a proton. The mutation of either H122 or E53 in bsSHMT does not affect the cleavage of L-*allo*-Thr, although the physiological activity of SHMT is completely abolished [7–10]. This shows that neither H122 nor E53 is involved in the abstraction of the proton from the side-chain hydroxyl group. The superposition of the bsSHMT–Gly–FTHF ternary complex with Y51F and the Y61A bsSHMT–L-*allo*-Thr complex shows that the additional methyl group at Cβ causes a severe steric clash with the FTHF molecule. This may prevent binding of FTHF/THF to SHMT when an L-*allo*-Thr external aldimine is formed, and cleavage occurs in the absence of THF.

Earlier studies have also shown that there is a linear relationship between the rate of THF-independent cleavage of β-substituted substrates and the hydration equilibrium of the product aldehyde, demonstrating that cleavage is accelerated by the presence of electron-donating substituents at Cβ [22]. It has been shown that, of the β-hydroxy amino acid substrates, L-Ser and α-methyl-L-Ser are the slowest reactants (10^5 fold slower) for SHMT in the absence of THF [22]. However, the question that still remains unanswered is why Y61 cannot abstract a Cα proton from L-Ser when THF is not present. It is probable that the hydroxyl group of L-Ser has a lower radius than the CH_3 group of L-*allo*-Thr, which facilitates higher hydration. This makes the Cα–Cβ bond energetically stable, and hence the removal of the Cα proton by Y61 is unfavourable.

The studies presented here show that the mutation of either Y51 or Y61 affects the THF-independent cleavage of L-*allo*-Thr (Table 1). An examination of the active site geometry in bsSHMT (Fig. 1) and the Y51F and Y61A mutants shows that Y51 and Y61 are not placed suitably for the removal of a proton from the hydroxyl group of L-*allo*-Thr. However, they may have a role in abstracting a proton from the Cα atom of L-*allo*-Thr. The hydroxyl group of Y51 is 3.6 and 3.8 Å from Cα of Gly and Ser, respectively, in bsSHMT. Of the two residues, Y51 is unlikely to be involved in proton abstraction from Cα of the bound ligand because of its greater distance and incorrect geometry. In contrast, the hydroxyl group of Y61 is 3.3 and 3.2 Å from Cα of Gly and Ser, respectively. Y61 may therefore be involved in Cα proton abstraction in the THF-independent reaction. The Y51 to F mutation leads to a change in the orientation of Y61 and increases the distance between the hydroxyl group of Y61 and Cα of the ligand. In Gly, L-Ser and L-*allo*-Thr complexes with Y51F bsSHMT, the hydroxyl group of Y61 and Cα of the bound ligand are at distances of 4.97, 4.39 and 4.39 Å, respectively. This may lead to the loss of L-*allo*-Thr cleavage activity of Y51F bsSHMT. It may therefore be concluded that Y51 is important for PLP binding and appropriate positioning of Y61, and Y61 is involved in the abstraction of the proton from the Cα carbon of L-*allo*-Thr. On the basis of these observations, a possible mechanism for the SHMT-catalysed cleavage of L-*allo*-Thr is suggested (Scheme 2).

In this mechanism (Scheme 2), after the formation of the L-*allo*-Thr external aldimine (**II**), cleavage is triggered by the abstraction of a Cα proton by Y61, leading to the formation of a carbanion intermediate (**III**). This is followed by an internal rearrangement of a proton from the side-chain hydroxyl group of L-*allo*-Thr to Cα, and concomitant cleavage of the Cα–Cβ bond. This bond cleavage leads to the release of acetaldehyde, leaving behind the Gly quinonoid intermediate (**IV**). Reprotonation of the quinonoid intermediate at C4 converts it into the Gly external aldimine (**V**). This is followed by the nucleophilic attack of the ε-amino group of the active site Lys on the Gly external aldimine, leading to the internal aldimine and the release of Gly. These results suggest that the catalysis of

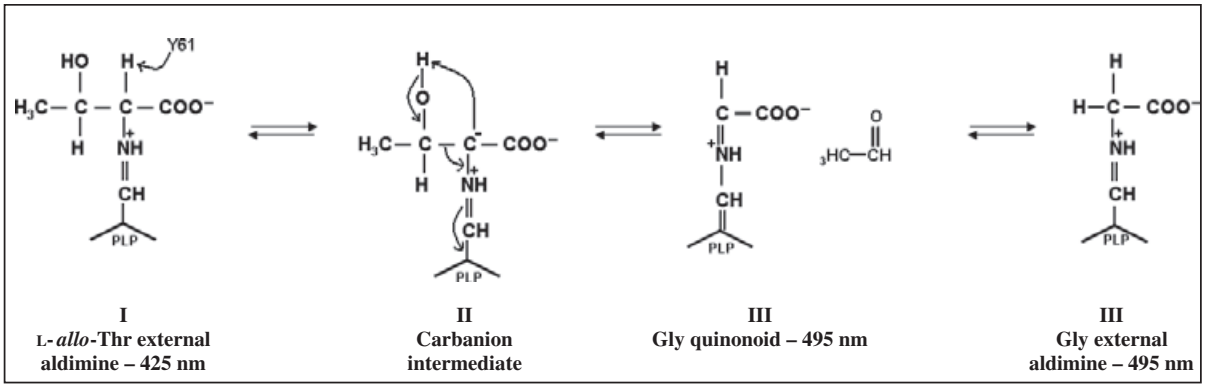

I
L-*allo*-Thr external aldimine – 425 nm

II
Carbanion intermediate

III
Gly quinonoid – 495 nm

III
Gly external aldimine – 495 nm

Scheme 2. Proposed mechanism for the cleavage of L-*allo*-Thr.

3-hydroxy amino acids could proceed via abstraction of a Cα proton rather than the hydroxyl proton by Y61 of bsSHMT.

Materials and methods

Site-directed mutagenesis

Plasmids were prepared by the alkaline lysis procedure using the DH5α strain of *Escherichia coli* [23]. The preparation of competent cells and transformation were carried out by the method of Alexander [24]. The Y51F bsSHMT mutant was constructed by a PCR-based sense–antisense primer method [25] with pRSH (bsSHMT gene cloned in pRSET C vector) as template using appropriate sense (5′-GACGAACAAA*TTC*GCGGAAGG-3′) and anti-sense (5′-CCTTCCGCGAATTTGTTCGTC-3′) primers and Deep Vent Polymerase (New England Biolabs, Beverly, MA, USA). The Y61F bsSHMT and Y61A bsSHMT mutants were also generated by a similar procedure using the following primers: Y61F (sense), 5′-GCCGCTAT*TTT* GGCGGCTGC-3′; Y6F (antisense), 5′-GCAGCCGCCA AAATAGCGGCG-3′; Y61A (sense), 5′-CGCCGCTAT*G CT*GGCGGCTGC-3′; Y6A (antisense), 5′-GCAGCCGCC AGCATAGCGGCG-3′. The nucleotides in italic indicate the mutation introduced. The mutations were confirmed by DNA sequencing.

Expression and purification of Y51F, Y61F and Y61A bsSHMTs

Y51F, Y61F and Y61A bsSHMT constructs were transformed into *E. coli* BL21 (DE3) pLysS strain. A single colony was grown at 30 °C in 50 mL of Luria–Bertani (LB) medium containing 50 $\mu g \cdot mL^{-1}$ ampicillin. These cells were inoculated into 1 L of terrific broth containing 50 $\mu g \cdot mL^{-1}$ ampicillin. After 3–4 h at 30 °C (A_{600} = 0.6), cells were induced with 0.3 mM isopropyl thio-β-D-galactoside for 4–5 h. The mutant enzymes were purified by a procedure identical to that used for the wild-type enzyme [26]. Briefly, the cells were harvested, resuspended in 60 mL of buffer A (50 mM potassium phosphate, pH 7.4, 2-mercaptoethanol, 1 mM EDTA and 100 μM PLP) and sonicated. The supernatant was subjected to 0–65% ammonium sulfate precipitation. The pellet obtained was resuspended in 20–30 mL of buffer B (20 mM potassium phosphate, pH 8.0, 1 mM 2-mercaptoethanol, 1 mM EDTA and 50 μM PLP) and dialysed for 24 h against the same buffer (1 L with two changes). The dialysed sample was loaded onto DEAE-cellulose previously equilibrated with buffer B. The column was washed with 500 mL of buffer B, and the bound protein was eluted with 50 mL of buffer C (200 mM potassium phosphate, pH 6.4, 1 mM EDTA, 1 mM 2-mercaptoethanol, 50 μM PLP). The eluted protein was precipitated at 65% ammonium sulfate saturation, and the pellet was resuspended in buffer D (50 mM potassium phosphate, pH 7.4, 1 mM EDTA, 1 mM 2-mercaptoethanol) and dialysed against the same buffer (2 L, with two changes) for 24 h. The purified proteins were homogeneous when examined using SDS-PAGE. Protein was estimated by the method of Lowry *et al.* [27] using BSA as the standard.

Enzyme assays

SHMT-catalysed THF-dependent cleavage of L-Ser to Gly and 5,10-methylene THF was monitored using L-[3-^{14}C]-Ser (Amersham Pharmacia Biotech Ltd, Little Chalfont, Buckinghamshire, UK) [28]. One unit of enzyme activity was defined as the amount of enzyme that catalyses the formation of 1 μmol of formaldehyde per minute at 37 °C. Specific activity was expressed as units per milligram of protein.

SHMT-catalysed THF-independent aldol cleavage of L-*allo*-Thr to Gly and acetaldehyde was monitored at 340 nm by the NADH-dependent reduction of acetaldehyde to ethanol and NAD^+ by alcohol dehydrogenase present in an excess amount in the reaction mixture [7]. NADH consumed in the reaction was calculated using a molar

extinction coefficient of 6220 $M^{-1}\cdot cm^{-1}$. Both THF-dependent and THF-independent SHMT reactions were carried out in duplicate using protein from three independent purifications. The kinetic constants were calculated using double reciprocal plots. The pseudo-first-order rate constant for the THF-independent transamination of D-Ala was calculated from the time course of the decrease in the absorption at 425 nm [7].

Spectroscopic methods

The visible absorption spectra were recorded on a JASCO V-530 UV/Visible spectrophotometer (Hachioji, Tokyo, Japan) in buffer D at 25 ± 2 °C using 1 $mg\cdot mL^{-1}$ (25 μM) of the enzyme. CD measurements were made in a Jasco J-500A automated recording spectropolarimeter. Spectra were collected at a scan speed of 10 $nm\cdot min^{-1}$ and a response time of 16 s. Visible CD spectra were recorded from 550 to 300 nm using a protein concentration of 1 $mg\cdot mL^{-1}$ in buffer D with or without substrates (L-Ser/Gly, THF/FTHF).

Estimation of PLP at the active site

The enzyme (1 $mg\cdot mL^{-1}$) was incubated with 0.1 M NaOH for 5 min. The PLP content was determined by measuring the absorbance at 388 nm assuming a molar absorption coefficient of 6600 $M^{-1}\cdot cm^{-1}$ for PLP [29].

Reduction with sodium cyanoborohydride ($NaCNBH_3$)

The wild-type, Y51F and Y61F bsSHMTs (1 $mg\cdot mL^{-1}$) were incubated with 1 mM $NaCNBH_3$, and the absorption spectra were recorded in the range 300–550 nm at 0, 5 and 30 min, respectively, at 37 °C. This treatment reduces the internal aldimine to a secondary amine [18].

Crystallization, data collection and processing

The pellet containing the enzyme obtained after final ammonium sulfate precipitation was resuspended in 100 mM Hepes pH 7.5 containing 0.2 mM EDTA and 5 mM 2-mercaptoethanol. Ammonium sulfate was removed and the buffer was changed from phosphate to Hepes by repeated concentration and dilution using an Amicon Centricon filter (Millipore, Bangalore, India). Crystals of Y51F and Y61A bsSHMT mutants were obtained by hanging drop vapour diffusion using 50% 2-methyl 2,4-pentanediol as the precipitant. However, it was not possible to obtain crystals of the Y61F mutant. The ligands (10 mM) (Gly/L-Ser/L-*allo*-Thr) were used to obtain crystals of the complexes. FTHF (2 mM) was incubated with the enzyme when required [6]. Crystals were soaked in the mother

Table 2. Data collection statistics for Y51F bsSHMT and its complexes. Values in parentheses correspond to the highest resolution shell.

Ligand(s) used	None	Gly	L-Ser	L-*allo*-Thr	Gly + FTHF	L-Ser + FTHF
Space group	$P2_12_12$	$P2_12_12$	$P2_12_12$	$P2_12_12$	$P2_12_12$	$P2_12_12$
Unit cell parameters						
a (Å)	61.25	60.92	61.01	60.93	61.05	61.01
b (Å)	106.54	106.39	106.51	106.28	106.47	106.44
c (Å)	57.29	57.02	57.17	57.04	57.18	57.11
Resolution range (Å)	30.0–1.80 (1.86–1.80)	30.0–1.69 (1.75–1.69)	30.0–1.66 (1.72–1.66)	30.0–1.92 (1.99–1.92)	30.0–1.66 (1.72–1.66)	30.0–1.66 (1.72–1.66)
Completion (%)	99.6 (100)	99.8 (100)	96.5 (83.7)	98.0 (99.5)	92.2 (81.4)	91.7 (81.4)
R_{merge} (%)	8.1 (46.2)	5.6 (49.8)	5.7 (45.3)	9.1 (48.4)	5.6 (45.5)	5.2 (32.3)
Total reflections	450 345	399 596	864 189	919 026	836 525	712 023
Unique reflections	35 330	41 824	43 037	28 280	41 138	40 845
$\langle I\rangle/\langle\sigma\rangle$	12.2 (2.7)	23.8 (2.8)	24.8 (3.8)	13.6 (3.2)	26.2 (3.5)	29.4 (5.7)
Wilson *B* ($Å^2$)	18.7	23.8	23.3	21.3	23.6	23.4

Table 3. Data collection statistics for Y61A bsSHMT and its complexes. Values in parentheses correspond to the highest resolution shell.

Ligand(s) used	None	Gly	L-Ser	L-*allo*-Thr	Gly + FTHF	Gly + FTHF	L-Ser + FTHF
Space group	$P2_12_12$	$P2_12_12$	$P2_12_12$	$P2_12_12$	$P2_12_12$	$P2_1$	$P2_1$
Unit cell parameters							
a (Å)	61.16	61.21	61.35	61.48	61.43	61.43	61.69
b (Å)	105.92	106.22	105.23	105.02	105.88	105.90	105.86
c (Å)	56.91	57.17	56.93	56.95	57.12	57.10 β = 90.39	57.14 β = 90.78
Resolution range (Å)	30.0–2.70 (2.80–2.70)	30.0–1.66 (1.72–1.66)	30.0–2.40 (2.49–2.40)	30.0–2.40 (2.49–2.40)	30.0–1.86 (1.93–1.86)	30.0–1.95 (2.02–1.95)	30.0–1.90 (1.97–1.90)
Completion (%)	97.2 (99.1)	97.8 (89.2)	93.6 (99.2)	98.1 (99.8)	97.1 (99.6)	92.4 (98.5)	98.6 (99.9)
R_{merge} (%)	14.4 (40.4)	6.4 (33.9)	8.3 (42.4)	11.0 (42.7)	6.3 (40.2)	9.8 (50.3)	6.5 (48.9)
Total reflections	267 275	426 528	458 209	312 892	414 805	671 518	636 609
Unique reflections	10 086	42 717	13 694	14 402	31 141	47 840	54 631
$\langle I/\sigma \rangle$	7.6 (3.5)	13.0 (3.2)	18.6 (4.5)	12.2 (4.2)	20.9 (3.8)	10.7 (2.6)	18.4 (2.7)
Wilson *B* (Å^2)	31.7	22.1	47.3	49.6	27.0	27.4	31.4

liquor for a few seconds before flash freezing in a stream of nitrogen at 100 K. Data were collected at liquid nitrogen temperature using a Rigaku (Tokyo, Japan) RU-200 rotating anode X-ray generator (Cu Kα radiation) on a MAR345 (Hamburg, Germany) image plate detector system. Data were indexed, scaled and integrated using Denzo and Scalepack of the HKL suite of programs (HKL Research Inc., Charlottesville, VA, USA) [30]. Data collection statistics for Y51F bsSHMT and Y61A bsSHMT are given in Tables 2 and 3, respectively.

Structure determination and refinement

The crystal structure of bsSHMT (1KKJ) was used as the initial model for the refinement of Y51F and Y61A bsSHMTs. Water and ligand molecules were removed from the model. Rigid body refinement followed by restrained positional refinement were carried out using REFMAC5 [31] of the CCP4 suite of programs [32]. Five per cent of the unique reflections were reserved for the calculation of free *R* and for the validation and monitoring of the progress of refinement [33]. The refinement statistics for Y51F bsSHMT and Y61A bsSHMT are given in Tables 4 and 5, respectively. Electron density was visualized using COOT [34]. Alternating cycles of refinement and model building were carried out to improve the model. Ligand and water molecules were added during the last few cycles of refinement. Crystals of the ligand complexes of Y51F and Y61A bsSHMTs with Gly, Ser and L-*allo*-Thr were refined in a similar manner to that described above, starting from bsSHMT–Gly (1KL1) as the initial model. Final structures were validated using PROCHECK [35]. Structures of different complexes were superposed and rmsds for the superpositions were calculated using the program ALIGN [36]. The program CONTACT was used to find the residues within hydrogen bonding distances. Figures were generated using PyMOL [37].

Acknowledgements

MRNM and HSS thank the Indian Council of Medical Research and Department of Biotechnology (DBT) of the Government of India for financial support. Diffraction data were collected at the X-ray facility for Structural Biology at the Molecular Biophysics Unit, Indian Institute of Science, supported by the Department of Science and Technology and DBT. We thank Babu and James for their help during data collection. VR and BSB thank the Council for Scientific and Industrial Research, Government of India, for the award of fellowships. We thank Dr K. N. Gurudutt (Food Safety and Analytical Quality Control Laboratory, Central Food Technical Research Institute) for helpful discussions regarding the mechanism.

Table 4. Refinement statistics for Y51F bsSHMT and its complexes.

Ligand(s) used	None	Gly	L-Ser	L-*allo*-Thr	Gly + FTHF	L-Ser + FTHF
Resolution (Å)	23.2–1.80	20.43–1.69	22.45–1.67	22.4–1.92	21.30–1.67	21.44–1.67
Final *R* (%)	16.8	17.0	18.0	16.8	18.4	18.7
Free *R* (%)	20.1	20.5	21.1	20.7	21.5	21.5
rmsd bond (Å)	0.012	0.010	0.012	0.013	0.010	0.010
rmsd angle (deg)	1.247	1.243	1.331	1.354	1.242	1.228
Chiral ($Å^3$)	0.086	0.082	0.088	0.093	0.083	0.081
Number of protein atoms	3124	3141	3141	3123	3125	3143
Number of ligand atoms	30	38	48	41	38	40
Number of water molecules	434	427	436	340	435	419
Average *B* factor ($Å^2$)						
Protein atoms	14.2	18.9	17.6	18.6	19.1	19.0
Ligand atoms	29.6	32.1	28.0	30.1	31.7	31.5
Water molecules	25.3	30.9	28.4	27.2	29.5	29.6
Ramachandran plot (%)						
Mostly allowed	93.7	94.0	93.7	92.3	92.6	94.0
Allowed	5.1	4.9	5.4	6.6	6.3	4.9
Generously allowed	0.3	0.3	0.3	0.6	0.3	0.6
Disallowed	0.9	0.9	0.6	0.6	0.9	0.6

Table 5. Refinement statistics for Y61A bsSHMT and its complexes.

Ligand(s) used	None	Gly	L-Ser	L-*allo*-Thr	Gly + FTHF
Resolution (Å)	23.19–2.72	22.24–1.68	23.88–2.42	23.10–2.41	21.47–1.86
Final *R* (%)	21.7	19.0	24.0	23.0	19.5
Free *R* (%)	28.1	20.9	29.2	29.2	23.4
rmsd bond (Å)	0.006	0.007	0.006	0.006	0.007
rmsd angle (deg)	0.888	1.026	0.873	0.881	1.033
Chiral ($Å^3$)	0.055	0.069	0.055	0.056	0.070
Number of protein atoms	3106	3140	3109	3109	3125
Number of ligand atoms	15	38	22	23	20
Number of water molecules	69	424	79	87	300
Average *B* factor ($Å^2$)					
Protein atoms	19.4	16.2	41.8	40.1	25.8
Ligand atoms	20.8	35.2	46.1	41.5	25.9
Water molecules	9.7	26.1	37.7	36.2	34.2
Ramachandran plot (%)					
Mostly allowed	91.7	93.4	93.4	92.0	93.4
Allowed	7.1	5.7	5.4	6.9	6.0
Generously allowed	0.6	0.3	0.6	0.6	0.0
Disallowed	0.6	0.6	0.6	0.6	0.6

References

1 Matthews RB & Drummond JT (1990) Providing one-carbon units for biological methylations: mechanistic studies on serine hydroxymethyltransferase, methylene-tetrahydrofolate reductase and methyltetrahydrofolate-homocysteine methyltransferase. *Chem Rev* **90**, 1275–1290.

2 Rao NA, Talwar R & Savithri HS (2000) Molecular organization, catalytic mechanism and function of serine hydroxymethyltransferase – a potential target for cancer chemotherapy. *Int J Biochem Cell Biol* **32**, 405–416.

3 Malkin LI & Greenberg DM (1964) Purification and properties of threonine or *allo*-threonine aldolase from rat liver. *Biochim Biophys Acta* **85**, 117–131.

4 Chen MS & Schirch LV (1973) Serine transhydroxymethylase. A kinetic study of the synthesis of serine in the absence of tetrahydrofolate. *J Biol Chem* **248**, 3631–3635.

5 Ulevitch RJ & Kallen RG (1977) Purification and characterization of pyridoxal 5′-phosphate dependent

serine hydroxymethylase from lamb liver and its action upon beta-phenylserines. *Biochemistry* **16**, 5342–5350.
6 Trivedi V, Gupta A, Jala VR, Saravanan P, Rao GSJ, Rao NA, Savithri HS & Subramanya HS (2002) Crystal structure of binary and ternary complexes of serine hydroxymethyltransferase from *Bacillus stearothermophilus*: insights into the catalytic mechanism. *J Biol Chem* **277**, 17161–17169.
7 Rao JV, Prakash V, Rao NA & Savithri HS (2000) The role of Glu74 and Tyr82 in the reaction catalyzed by sheep liver cytosolic serine hydroxymethyltransferase. *Eur J Biochem* **267**, 5967–5976.
8 Rajaram V, Bhavani BS, Kaul P, Prakash V, Rao NA, Savithri HS & Murthy MRN (2007) Structure determination and biochemical studies on *Bacillus stearothermophilus* E53Q serine hydroxymethyltransferase and its complexes provide insights on function and enzyme memory. *FEBS J* **274**, 4148–4160.
9 Szebenyi DM, Musayev FN, di Salvo ML, Safo MK & Schirch V (2004) Serine hydroxymethyltransferase: role of Glu75 and evidence that serine is cleaved by a retro-aldol mechanism. *Biochemistry* **43**, 6865–6876.
10 Jagath JR, Sharma B, Rao NA & Savithri HS (1997) The role of His-134, -147, and -150 residues in subunit assembly, cofactor binding, and catalysis of sheep liver cytosolic serine hydroxymethyltransferase. *J Biol Chem* **272**, 24355–24362.
11 Ziak M, Jager J, Malashkevich VN, Gehring H, Jaussi R, Jansonius JN & Christen P (1993) Mutant aspartate aminotransferase (K258H) without pyridoxal-5′phosphate-binding lysine residue – structural and catalytic properties. *Eur J Biochem* **211**, 475–484.
12 Toney MD & Kirsch JF (1991) Tyrosine 70 fine-tunes the catalytic efficiency of aspartate aminotransferase. *Biochemistry* **30**, 7456–7461.
13 Tan D, Barber MJ & Ferreira GC (1998) The role of tyrosine 121 in cofactor binding of 5-aminolevulinate synthase. *Protein Sci* **7**, 1208–1213.
14 Sun S & Toney MD (1999) Evidence for a two-base mechanism involving tyrosine-265 from arginine-219 mutants of alanine racemase. *Biochemistry* **38**, 4058–4065.
15 Bhavani S, Trivedi V, Jala VR, Subramanya HS, Kaul P, Prakash V, Appaji Rao N & Savithri HS (2005) Role of Lys-226 in the catalytic mechanism of *Bacillus stearothermophilus* serine hydroxymethyltransferase – crystal structure and kinetic studies. *Biochemistry* **44**, 6929–6937.
16 Contestabile R, Angelaccio S, Bossa F, Wright HT, Scarsdale N, Kazanina G & Schirch V (2000) Role of tyrosine 65 in the mechanism of serine hydroxymethyltransferase. *Biochemistry* **39**, 7492–7500.
17 Schirch V & Szebenyi DM (2005) Serine hydroxymethyltransferase revisited. *Curr Opin Chem Biol* **9**, 482–487.
18 Schirch D, Delle FS, Iurescia S, Angelaccio S, Contestabile R, Bossa F & Schirch V (1993) Serine hydroxymethyltransferase: role of the active site lysine in the mechanism of the enzyme. *J Biol Chem* **268**, 23132–23138.
19 David D, Rozanne P & Olga A (1986) Cytidine diphosphate 4-keto-6-dioxy-d-glucose-3-dehydrogenase. In *Coenzymes and Cofactors, Vitamin B6 Pyridoxal Phosphate – Chemical, Biochemical and Medical Aspects* (David D, Rozanne P & Olga A, eds), pp. 392–418. John Wiley & Sons, Hoboken, NJ.
20 Acharya JK, Prakash V, Rao AGA, Savithri HS & Rao NA (1991) Interactions of methoxyamine with pyridoxal-5′-phosphate–Schiff's base at the active site of sheep liver serinehydroxymethyltransferase. *Indian J Biochem Biophys* **28**, 381–388.
21 Jala VR, Ambili M, Prakash V, Rao NA & Savithri HS (2003) Disruption of distal interactions of Arg 262 and of substrate binding to Ser 52 affect catalysis of sheep liver cytosolic serine hydroxymethyltransferase. *Indian J Biochem Biophys* **40**, 226–237.
22 Webb HK & Matthews RG (1995) 4-Chlorothreonine is substrate, mechanistic probe, and mechanism-based inactivator of serine hydroxymethyltransferase. *J Biol Chem* **270**, 17204–17209.
23 Studier FW & Moffatt BA (1986) Use of bacteriophage T7 RNA polymerase to direct selective high-level expression of cloned genes. *J Mol Biol* **189**, 113–130.
24 Alexander DC (1987) An efficient vector-primer cDNA cloning system: large scale preparation of competent cells. *Methods Enzymol* **154**, 41–64.
25 Weiner MP, Costa GL, Schoetglin W, Cline J, Mathur E & Bauer JC (1994) Site directed mutagenesis of double-stranded DNA by the polymerase chain reaction. *Gene* **151**, 119–123.
26 Jala VR, Prakash V, Rao NA & Savithri HS (2002) Overexpression and characterization of dimeric and tetrameric forms of recombinant serine hydroxymethyltransferase from *Bacillus stearothermophilus*. *J Biosci* **27**, 233–242.
27 Lowry OH, Rosebrough NJ, Farr AL & Randall RJ (1951) Protein measurement with the Folin phenol reagent. *J Biol Chem* **193**, 265–275.
28 Taylor RT & Weissbach H (1965) A radioactive assay for serine hydroxymethyltransferase. *Anal Biochem* **13**, 80–84.
29 Peterson EA & Sober HA (1954) Preparation of crystalline phosphorylated derivatives of vitamin B6. *J Am Chem Soc* **76**, 169–183.
30 Otwinowsky Z & Minor W (1997) Processing of X-ray diffraction data collected in oscillation mode. *Methods Enzymol* **276**, 307–326.
31 Murshudov GN, Vagin AA & Dodson EJ (1997) Refinement of macromolecular structures by the maximum-likelihood method. *Acta Crystallogr D Biol Crystallogr* **53**, 240–255.

32 CCP4 (1994) The CCP4 suite: programs for protein crystallography. *Acta Crystallogr D Biol Crystallogr* **50**, 760–763.
33 Brunger AT (1993) Assessment of phase accuracy by cross validation: the free R value. Methods and applications. *Acta Crystallogr D Biol Crystallogr* **49**, 24–36.
34 Emsley P & Cowtan K (2004) COOT: model-building tools for molecular graphics. *Acta Crystallogr D Biol Crystallogr* **60**, 2126–2132.
35 Laskowski RA, McArthur MW, Moss DS & Thornton JM (1993) PROCHECK: a program to check the stereo-chemical quality of protein structures. *J Appl Crystallogr* **26**, 283–291.
36 Cohen GE (1997) ALIGN: a program to superimpose protein coordinates accounting for insertions and deletions. *J Appl Crystallogr* **30**, 1160–1161.
37 DeLano WL (2002) *The PYMOL Molecular Graphics System*. DeLano Scientific, San Carlos, CA.